



Insights Into MRI Neuroimaging Patterns of COVID-19 in Children: A Retrospective Comprehensive Analysis

Mohamad Gamal Nada, Yassir Edrees Almalki, Mohammad Abd Alkhalik Basha¹, Maha Ibrahim Metwally, Riham Dessouky, Mohamed Hesham Saleh Saleh Radwan, Mohamed M.A. Zaitoun, Ahmed A. El-Hamid M. Abdalla, Ahmed A.A. Bessar, Engy Fathy Tantwy, Mostafa Mohamad Assy, Bassant Mahmoud Dawoud, Diana Hanna, Mahmoud M. Gohary, Sharifa Khalid Alduraibi, Alaa K. Iduraibi, Diaa Bakry Eldib, Hamada M. Khater, Noha T. Sarhan, Dina Esmat Hamed, Sara F. Saadawy, Mohammed A. Huneif, Ahmed M. Abdelkhalik Basha, Yasmin Ibrahim Libda

Rationale and Objectives: Neurological complications associated with coronavirus disease (COVID-19) have been reported in children; however, data on neuroimaging findings remain limited. This study aimed to comprehensively examine neuroimaging patterns of COVID-19 in children and their relationship with clinical outcomes.

Materials and Methods: This retrospective cross-sectional study involved reviewing the medical records and MRI scans of 95 children who developed new neurological symptoms within 2–4 weeks of clinical and laboratory confirmation of COVID-19. Patients were categorized into four groups based on guidelines approved by the Centers for Disease Control and Prevention (CDC). Initial brain/spinal MRI was performed. Images were reviewed by three blinded radiologists, and the findings were analyzed and categorized based on the observed patterns in the brain and spinal cord. Follow-up MRI was performed and analyzed to track lesion progression.

Results: Encephalopathy was the most common neurological symptom (50.5%). The most common initial MRI involvement patterns were non-confluent multifocal hyperintense white matter (WM) lesions (36.8%) and ischemia (18.9%). Most patients who underwent follow-up MRI ($n = 56$) showed complete resolution (69.9%); however, some patients developed encephalomalacia and myelomalacia (23.2% and 7.1%, respectively). Non-confluent hyperintense WM lesions were associated with good outcomes (45.9%, $P = 0.014$), whereas ischemia and hemorrhage were associated with poor outcomes (44.1%, $P < 0.001$).

Conclusion: This study revealed diverse neuroimaging patterns in pediatric COVID-19 patients. Non-confluent WM lesions were associated with good outcomes, whereas ischemia and hemorrhage were associated with poorer prognoses. Understanding these patterns is crucial for their early detection, accurate diagnosis, and appropriate management.

Key Words: COVID-19; Neurological manifestations; Neuroimaging; MRI; Children.

© 2024 The Association of University Radiologists. Published by Elsevier Inc. All rights are reserved, including those for text and data mining, AI training, and similar technologies.

Acad Radiol 2024; 31:2536–2549

From the Department of Diagnostic Radiology, Faculty of Human Medicine, Zagazig University, Zagazig, Egypt (M.G.N., M.A.A.B., M.I.M., R.D., M.H.S.S.R., M.M.Z., A.-H.A., A.A.B., E.F.T., M.M.A., Y.I.L.); Division of Radiology, Department of Internal Medicine, Medical College, Najran University, Najran, Kingdom of Saudi Arabia (Y.E.A.); Department of Diagnostic Radiology, Faculty of Human Medicine, Tanta University, Tanta, Egypt (B.M.D.); Pediatric Department, Faculty of Human Medicine, Zagazig University, Zagazig, Egypt (D.H., M.M.G.); Department of Radiology, College of Medicine, Qassim University, Buraidah, Kingdom of Saudi Arabia (S.K.A., A.K.I.); Department of Radiology, Faculty of Human Medicine, Benha University, Benha, Egypt (D.B.E., H.M.K.); Department of Neurology, Faculty of Human Medicine, Zagazig University, Zagazig, Egypt (N.T.S.); Department of Dermatology, Venereology, and Andrology, Faculty of Human Medicine, Zagazig University, Zagazig, Egypt (D.E.H.); Medical Biochemistry Department, Faculty of Human Medicine, Zagazig University, Zagazig, Egypt (S.F.S.); Pediatric Department, Medical College, Najran University, Najran, Saudi Arabia (M.A.H.); Faculty of General Medicine, St. Petersburg State University, Egypt Branch, Cairo, Egypt (A.M.A.B.). Received February 6, 2024; revised March 16, 2024; accepted March 17, 2024. **Address correspondence to:** M.A.A.B. e-mail: Mohammad_basha76@yahoo.com, Maatya@zu.edu.eg

¹ ORCID iD: 0000-0002-9075-8020

© 2024 The Association of University Radiologists. Published by Elsevier Inc. All rights are reserved, including those for text and data mining, AI training, and similar technologies.

<https://doi.org/10.1016/j.acra.2024.03.018>

INTRODUCTION

The coronavirus disease 2019 (COVID-19) pandemic has affected millions of individuals worldwide. Although adults appear to be more susceptible to severe infections, children are not spared from this disease (1). There is increasing evidence that COVID-19 can lead to neurological complications in both adults and children (2). In children and even neonates, cases of neurological involvement associated with both the acute and delayed phases of COVID-19 have developed. Incidence rates vary between 3.8% and 43%, suggesting a potentially higher neurological impact in the pediatric population (3–8). In children, the temporal progression of COVID-19 can evolve into an inflammatory process during the latent phase, known as the multisystem inflammatory syndrome in children (MIS-C). MIS-C is characterized by fever, involvement of multiple organ systems, laboratory abnormalities, and exposure to COVID-19 within 2–4 weeks prior to symptom onset (9,10).

Neuroimaging techniques, such as magnetic resonance imaging (MRI) and computed tomography (CT), have been utilized to assess the neurological impact of COVID-19 in different populations, including children (11). Several studies have reported neuroimaging findings in children with COVID-19, providing insight into how this disease affects the developing brain. These studies revealed a range of findings, including diffuse cerebral edema, white matter (WM) hyperintensities, ischemic strokes, hemorrhagic lesions, leukoencephalopathy, and encephalitis. Although these findings are based on a limited number of patients, they highlight the importance of continued research to better understand the long-term effects of COVID-19 on children's developing brains (6,7,12–16).

Understanding the neuroimaging findings of COVID-19 in children is crucial for the early detection, accurate diagnosis, and appropriate management of neurological complications. This knowledge can aid in providing targeted interventions and improving the overall outcomes in affected pediatric patients (13,17,18). This study aimed to comprehensively examine neuroimaging patterns of COVID-19 in children and their relationship with clinical outcomes.

MATERIALS AND METHODS

Study Population

Between October 2020 and October 2023, we conducted a three-year retrospective review of the medical records and MRI scans archived at our hospital. The goal was to study children aged 18 years or younger who developed new neurological symptoms within 2–4 weeks of a documented laboratory-confirmed COVID-19 infection. Patients with preexisting comorbidities documented in their records such as neurological or neurodevelopmental disorders (e.g., epilepsy, cerebral palsy, leukodystrophies), major chronic systemic diseases that could impact neurological function

(e.g., malignancies, collagen vascular diseases), and positive tests confirming co-infection with other organisms, were excluded from the analysis. Additional exclusion criteria are shown in Figure 1. After applying the eligibility criteria, 95 pediatric patients were included in the final study.

Clinical Categorization

We used a categorization scheme that incorporated temporal, clinical, and laboratory factors to classify the clinical course of COVID-19, following the guidelines described by Lindan et al. (6). Two pediatricians (BLINDED) and one neurologist (BLINDED), with over 10 years of experience in pediatric neurology, reviewed the patients' admission sheets, medical records, laboratory results, discharge sheets, and follow-up visits. The patients were then classified into four categories according to the Centers for Disease Control and Prevention (CDC)-approved guidelines: category 1 (symptomatic acute COVID-19 infection), category 2 (asymptomatic acute or subacute COVID-19 infection), category 3 (MIS-C), and category 4 (indeterminate) (Fig 1). Patients categorized as acute, subacute, or indeterminate did not meet CDC criteria for MIS-C. Age, sex, and primary symptoms (general, respiratory, neurological, gastrointestinal, and other concomitant symptoms) were recorded for each category. The duration of hospitalization, treatment received, need for intubation, and outcomes were also reported.

MRI Protocol

All MRI scans were conducted in our department using a 1.5 T scanner (Achieva, Philips Medical System, Best, The Netherlands) and an eight-channel head coil. Our standard protocol for pediatric brain imaging included pre-contrast axial T1-weighted turbo spin echo (T1W TSE) (TE = 10–12 ms, TR = 400–600 ms), axial and coronal T2W TSE (TE = 70–90 ms, TR = 2800–3500 ms), axial and sagittal fluid-attenuated inversion recovery (FLAIR) imaging (TE = 80–140 ms, TR = > 6000 ms, TI = 200 ms), T2*W fast field echo (TR = 600–755 ms, TE = 18–23 ms, flip angle 10–18), diffusion-weighted imaging (DWI) (TE = 86 ms, TR = 5000 ms) with b values of 0 and 1000 s/mm², and apparent diffusion coefficient (ADC) mapping. Additional post-contrast T1W sequences were obtained after administration of intravenous gadolinium DTPA (0.2 mL/kg) in the axial, sagittal, and coronal planes. For spinal imaging, axial and sagittal T1W TSE (TE = 10–20 ms, TR = 400–600 ms), axial and coronal T2W TSE (TE = 70–90 ms, TR = 2500–4000 ms), axial and sagittal FLAIR (TE = 80–140 ms, TR ≥ 6000 ms, TI = 200 ms), DWI (TE = 12000 ms, TR = 95 ms, TI = 2200 ms) with b values of 800 and 1000 s/mm², and post-contrast axial and sagittal T1W sequences were obtained. All sequences were performed with a slice thickness = 2–3 mm, gap = 1 mm, FOV = 16–30 cm, and matrix = 512 × 512. For pediatric patients requiring sedation or anesthesia during MRI

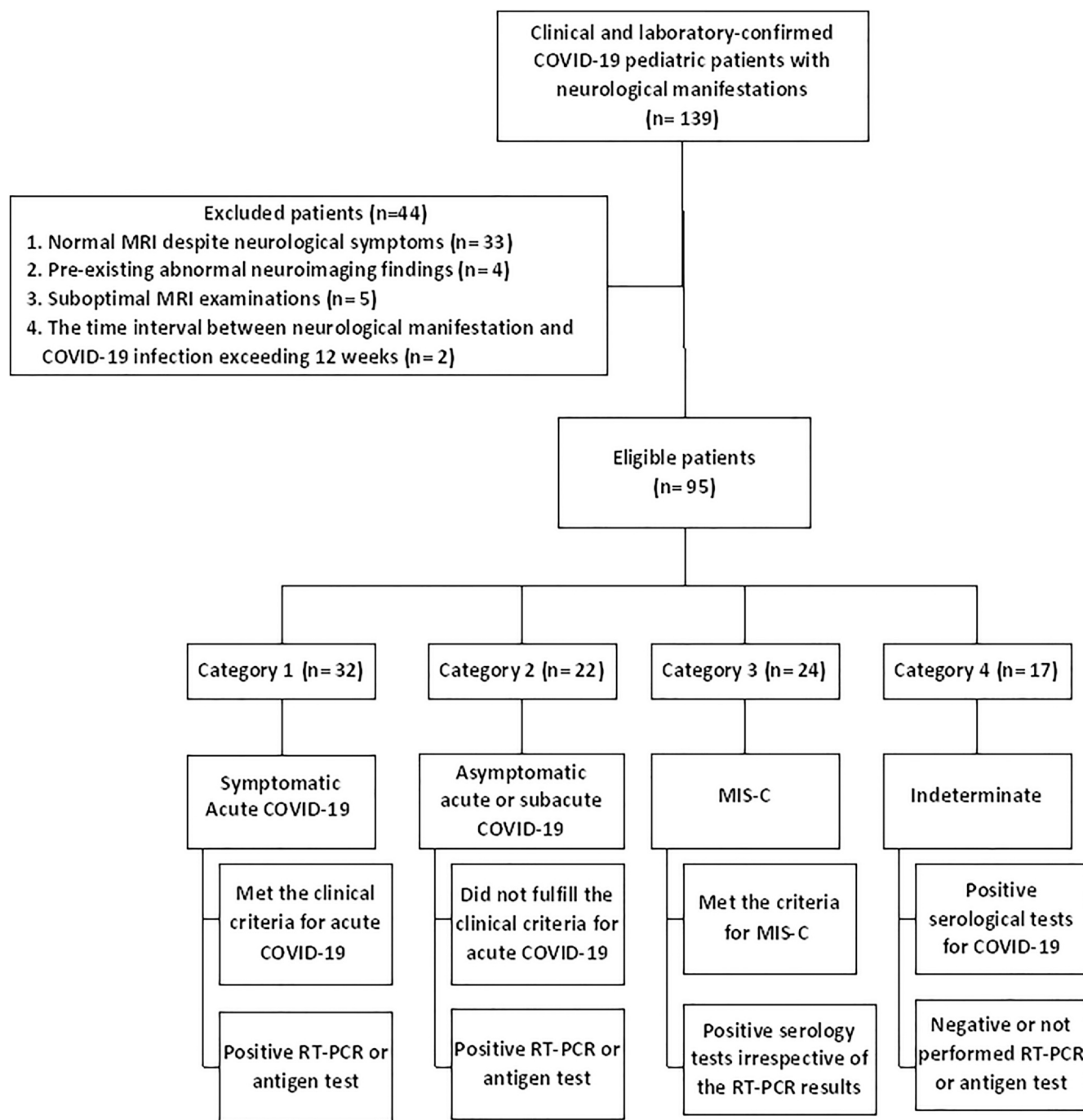


Figure 1. Flowchart of the study.

examinations, appropriate measures were taken to ensure their safety and comfort. Sedation or anesthesia protocols were followed according to institutional guidelines and in consultation with the pediatric anesthesia team to minimize any potential risks or discomfort to the children during the procedure.

MR Image Analysis

A panel of three radiologists (BLINDED) with over 10 years of experience in neuroimaging, blinded to clinical information and

categorization, independently interpreted each MRI examination. Any discrepancies in imaging assessment were resolved through re-review and consensus adjudication. T1W, T2W, and FLAIR images were reviewed for WM lesions in terms of laterality (unilateral or bilateral) and pattern of involvement (extensive and confluent multifocal WM hyperintense lesions, non-confluent multifocal WM hyperintense lesions, or isolated temporal lobe involvement). The nuclei of the deep gray matter, cerebellum/cerebellar peduncles, brainstem, splenium of the corpus callosum, and cranial nerves were also examined for

laterality and pattern of involvement. T1W and T2 * W were assessed to detect any intra-axial (microhemorrhage or intracerebral hematoma) or extra-axial hemorrhage. DWI and ADC maps were analyzed for signs of acute ischemic lesions and areas of restricted diffusion. Post-contrast images were used to identify abnormal cerebral or cranial nerve enhancements. Acute necrotizing encephalopathy was defined by the presence of characteristic symmetric thalamic T2/FLAIR hyperintensity associated with internal hemorrhage. Posterior reversible encephalopathy syndrome (PRES) was recorded based on the presence of preferential posterior cerebral parieto-occipital WM edema, considering the possibility of more extensive edema. Spinal MRI scans were assessed for the presence of myelitis with or without hemorrhage as well as to identify any abnormal cauda equina enhancement. Patients with follow-up MRI scans available in the archive were analyzed to interpret the temporal resolution and progression of various lesions, such as encephalomalacia, myelomalacia, cortical laminar necrosis, and gliosis.

Statistical Analysis of the Data

Data were entered into the computer and analyzed using the IBM SPSS software package (version 26.0; Armonk, NY, IBM Corp.). Categorical data were presented as numbers and percentages. The chi-square test was applied to compare the groups. Alternatively, Fisher's exact test was applied if more than 20% of the cells had an expected count of less than five. Continuous data were tested for normality using the Kolmogorov–Smirnov test. Quantitative data were expressed as range (minimum and maximum), mean, standard deviation, and median. For non-normally distributed quantitative variables, the Mann–Whitney test was used to compare the groups. Fleiss kappa (κ) statistics for multiple raters were applied to evaluate the inter-rater agreement (IRA) of the various MR imaging patterns. The κ values were interpreted as follows: 0.01–0.20 = poor agreement; 0.21–0.40 = fair agreement; 0.41–0.60 = moderate agreement; 0.61–0.80 = good agreement; and 0.81–1.0 = perfect agreement. The significance of the results was determined at a P -value < 0.05.

RESULTS

Demographic and Clinical Features of the Patient Population

95 patients were enrolled in our study (mean age, 8.2 ± 4.2 ; age range, 4 months to 16.2 years; 53.7% female and 46.3% male). The predominant neurological symptom was encephalopathy (50.5%), followed by weakness and movement disorders (34.7%), headache (33.7%), and seizures (23.2%). [Table 1](#) displays the basic demographic and clinical features of the patients in the different categories.

Initial MRI Involvement Pattern

Initial MRI scans were conducted within 1–11 days after the onset of neurological symptoms (mean, 3.02 ± 2.29 days).

[Table 2](#) shows the initial MRI involvement patterns of the brain and spinal cord in the different categories. The most common pattern observed was non-confluent multifocal hyperintense lesions in the WM on FLAIR sequences (36.8%). This pattern was consistently observed in all clinical categories. The second most common pattern was ischemia (18.9%). Other identified patterns included extensive and confluent hyperintense WM lesions on FLAIR (11.6%), cranial nerve enhancement (10.5%), isolated temporal lobe involvement (6.3%), PRES (2.1%), and acute necrotizing encephalopathy (3.2%). Hemorrhages were observed in 21.1% of patients, with microhemorrhages being the most common form (14.7%). Isolated hemorrhages were found as a separate pattern in one patient, whereas in other patients, they occurred alongside other patterns. Diffusion restriction was found in 45.3% of patients, being present in all patients with ischemia and occurring in 26.3% of patients as foci of diffusion restriction, together with other patterns. Myelitis was present in 15.8% of patients, while cauda equina and nerve root enhancement (Guillain–Barre syndrome) were seen in 12.6% of patients. Of the patients with myelitis, 33.3% showed isolated spinal cord lesions, whereas the remaining 66.7% showed non-confluent multifocal FLAIR lesions with high signals in the WM. Three patients with cauda equina and nerve root enhancement had cytotoxic lesions in the splenium of the corpus callosum. Two of these patients were categorized as having MIS-C, and the third belonged to the indeterminate group.

Follow-up MRI Findings

Follow-up MRI scans were performed within 21–141 days following the onset of neurological symptoms, with a mean interval of 72.9 ± 31.4 days. Of the 95 patients enrolled in the study, only 56 underwent a follow-up MRI. Among these, 39 patients exhibited complete regression of previously observed imaging findings, 13 developed encephalomalacia, and four developed myelomalacia ([Table 3](#)).

IRA for Various MRI Involvement Patterns

The data presented in [Table 4](#) highlights the IRA for various MRI involvement patterns. Overall, the κ values indicated a high level of agreement, ranging from good to perfect. Overall brain MRI involvement patterns showed perfect agreement ($\kappa = 0.902$). Specific patterns such as acute necrotizing encephalopathy, PRES, isolated hemorrhage, and splenium of the corpus callosum involvement exhibit perfect agreement ($\kappa = 1.000$). In contrast, patterns such as cranial nerve enhancement and subarachnoid hemorrhage showed relatively lower κ values (0.781 and 0.796, respectively), yet still indicated good agreement. Spinal MRI and follow-up MRI patterns also showed perfect agreement ($\kappa = 0.918$ and 0.906, respectively).

Relation Between the Initial MR Involvement Patterns and Outcomes

Ischemia and hemorrhage had significantly higher rates of poor outcomes (44.1% for both; $P < 0.001$). Acute necrotizing

TABLE 1. Basic Demographic and Clinical Features of Patients in Different Categories

Variable	Total (n = 95)	Category 1 (n = 32)	Category 2 (n = 22)	Category 3 (n = 24)	Category 4 (n = 17)
Sex					
Male	44 (46.3)	14 (43.8)	8 (36.4)	12 (50)	10 (58.8)
Female	51 (53.7)	18 (56.3)	14 (14)	12 (50)	7 (41.2)
Age (years)					
Mean ± SD	8.2 ± 4.2	7.1 ± 4.8	9.4 ± 4.4	9.1 ± 3.4	7.1 ± 3.3
Median (Range)	8.0 (0.4–16.2)	5.8 (0.4–16)	10.0 (1.5–16.0)	10.0 (2–15)	7.0 (2.1–14.0)
Symptoms					
<i>Neurological symptoms</i>					
Headache	32 (33.7)	12 (37.5)	3 (13.6)	14 (58.3)	3 (17.6)
Seizures	22 (23.2)	8 (25)	4 (18.2)	7 (29.2)	3 (17.6)
Encephalopathy	48 (50.5)	16 (50)	7 (31.8)	9 (52.9)	8 (47.1)
Limb weakness and movement disorders	33 (34.7)	12 (37.5)	8 (36.4)	7 (29.2)	6 (35.3)
Cranial nerve affection	10 (10.5)	5 (15.6)	2 (9.1)	1 (4.2)	2 (11.8)
<i>General symptoms</i>					
Fever	63 (66.3)	30 (93.8)	9 (40.9)	24 (100)	–
Hypertension	1 (1.1)	1 (3.1)	0 (0.0)	0 (0)	–
Hypotension	7 (7.4)	0 (0)	0 (0.0)	7 (29.2)	–
<i>Respiratory symptoms</i>	46 (48.4)	31 (96.7)	0 (0.0)	15 (62.5)	–
<i>Gastrointestinal symptoms</i>	20 (21.1)	5 (15.6)	5 (22.7)	10 (41.7)	0 (0)
<i>Cutaneous rash</i>	10 (10.5)	0 (0)	0 (0.0)	10 (41.7)	–
Management					
<i>Duration of hospitalization (days)</i>					
Mean ± SD	15.7 ± 8.1	17.9 ± 10.6	13.5 ± 5.1	15.5 ± 7.1	14.5 ± 6.6
Median (Range)	14.0 (6–49)	14.0 (6–49)	14.0 (7–28)	13.5 (8–41)	11.0 (8–28)
<i>Mechanical ventilation</i>	30 (31.6)	11 (34.4)	4 (18.2)	14 (58.3)	1 (5.9)
<i>Immune modulation</i>					
IVIg	45 (47.4)	11 (34.4)	7 (31.8)	17 (70.8)	10 (58.8)
Steroids	70 (73.7)	21 (65.6)	15 (68.2)	23 (25.8)	11 (64.7)
<i>Anti-coagulation</i>	24 (25.3)	5 (15.6)	5 (22.7)	10 (41.7)	4 (23.5)
Outcome					
Good outcome	61 (64.2)	17 (53.1)	17 (77.3)	13 (54.2)	14 (82.4)
Poor outcome	23 (24.2)	10 (31.3)	4 (18.2)	6 (25)	3 (17.6)
Death	11 (11.6)	5 (15.6)	1 (4.5)	5 (20.8%)	0 (0)

Unless otherwise indicated, data represent the number of patients with percentages in parenthesis. IVIG, intravenous immunoglobulin; SD, Standard deviation.

encephalopathy was also significantly associated with poor outcomes (8.8%, $P < 0.043$). Diffusion restriction was associated with poor outcomes (67.7%; $P < 0.001$). However, when ischemia was excluded, foci with diffusion restrictions associated with other MRI patterns showed no significant difference between good and poor outcomes ($P < 0.893$). In contrast, non-confluent multifocal hyperintense WM lesions on FLAIR sequences were associated with good outcomes (45.9%, $P = 0.014$) (Table 5).

Figures 2–5 show representative cases from our study.

DISCUSSION

The findings of this study provide valuable insights into the neuroimaging patterns of pediatric patients who develop neurological symptoms following COVID-19 infection. To

the best of our knowledge, this is one of the few studies to comprehensively examine neuroimaging features in pediatric patients following COVID-19 infection. Our findings contribute to the growing body of literature on the neurological complications associated with COVID-19 in children. Understanding the neurological impact of COVID-19 in children is crucial for the early detection, accurate diagnosis, and effective management of complications.

The most common neurological symptom observed in our study was encephalopathy, which is consistent with previous reports (13,19). Encephalopathy is a broad term encompassing various neurological dysfunctions that can manifest as altered mental status, cognitive impairment, or behavioral changes. The underlying mechanisms leading to encephalopathy in COVID-19 are not yet fully understood but may involve direct viral invasion, immune-mediated processes, or vascular complications (20).

TABLE 2. Initial Brain and Spinal Cord MRI Involvement Patterns of the Different Categories

Findings	Total (n = 95)	Category 1 (n = 32)	Category 2 (n = 22)	Category 3 (n = 24)	Category 4 (n = 17)
Time to initial MRI (days)					
Mean ± SD	3.0 ± 2.3	2.3 ± 1.7	2.6 ± 1.8	3.9 ± 2.7	3.8 ± 2.7
Median (Range)	2 (1–11)	2 (1–8)	2 (1–8)	4 (1–10)	3 (1–11)
Initial brain MRI involvement patterns					
<i>WM involvement patterns</i>					
Extensive and confluent hyperintense WM lesions on FLAIR	11 (11.6)	3 (9.4)	2 (9.1)	4 (16.7)	2 (11.8)
Non-confluent multifocal hyperintense WM lesions on FLAIR	35 (36.8)	8 (25)	10 (45.5)	10 (41.7)	7 (41.2)
Isolated temporal lobe involvement	6 (6.3)	1 (3.1)	1 (4.5)	2 (8.3)	2 (11.8)
<i>Specific cerebral involvement patterns</i>					
Acute necrotizing encephalopathy	3 (3.2)	2 (6.3)	1 (4.5)	0 (0)	0 (0)
PRES	2 (2.1)	2 (6.3)	0 (0)	0 (0)	0 (0)
<i>Other involvement patterns</i>					
Ischemia	18 (18.9)	8 (25)	3 (13.6)	5 (20.8)	2 (11.8)
Cranial nerve enhancement	10 (10.5)	5 (15.6)	2 (9.1)	1 (4.2)	2 (11.8)
Isolated hemorrhage	1 (1.1)	0 (0)	1 (4.5)	0 (0)	0 (0)
<i>Concomitant MRI involvement patterns</i>					
Basal ganglia involvement	24 (25.3)	9 (28.1)	9 (40.9)	4 (16.7)	2 (11.8)
Brain stem involvement	26 (27.4)	11 (34.4)	6 (27.3)	5 (20.8)	5 (29.4)
Cerebellum involvement	21 (22.1)	12 (37.5)	4 (18.2)	3 (12.5)	2 (11.8)
Splenium of corpus callosum involvement	25 (26.3)	7 (21.9)	4 (18.2)	13 (54.2)	1 (5.9)
Diffusion restriction	43 (45.3)	13 (40.6)	8 (36.4)	17 (70.8)	5 (29.4)
Hemorrhage	20 (21.1)	11 (34.4)	3 (13.6)	4 (16.7)	2 (11.8)
Microhemorrhages	14 (14.7)	8 (25)	2 (9)	3 (12.5)	1 (5.9)
Intracerebral hematoma	4 (4.2)	2 (6.3)	1 (4.5)	1 (4.2)	0 (0)
Subarachnoid hemorrhage	2 (2.1)	1 (3.1)	0 (0)	0 (0)	1 (5.9)
Initial spinal MRI involvement patterns					
<i>Myelitis</i>					
Isolated myelitis without cerebral WM involvement	15 (15.8)	5 (15.6)	5 (22.7)	3 (12.5)	2 (11.8)
Myelitis associated with cerebral WM involvement	5 (5.3)	3 (9.4)	2 (9.1)	0 (0)	0 (0)
<i>Cauda equina and nerve roots enhancement</i>					
	10 (10.5)	2 (6.3)	3 (13.6)	3 (12.5)	2 (11.8)
	12 (12.6)	3 (9.4)	2 (9.1)	2 (8.3)	5 (29.4)

Unless otherwise indicated, data represent the number of patients with percentages in parenthesis. FLAIR, fluid-attenuated inversion recovery; MRI, magnetic resonance imaging; PRES, Posterior reversible encephalopathy syndrome; SD, Standard deviation; WM, white matter.

TABLE 3. Follow-up MRI Findings of the Different Categories

Findings	Total (n = 56)	Category 1 (n = 17)	Category 2 (n = 14)	Category 3 (n = 16)	Category 4 (n = 9)
Time to follow-up MRI, days, Mean \pm SD (Range)	72.9 \pm 31.4 (21–141)	67.9 \pm 32.9 (21–136)	72.6 \pm 31.7 (26–141)	75.4 \pm 33.0 (29–127)	78.4 \pm 28.8 (31–121)
Resolution	39 (69.9)	9 (52.9)	10 (71.4)	12 (75)	8 (88.9)
Encephalomalacia/atrophy	13 (23.2)	6 (35.3)	3 (21.4)	4 (25)	0 (0)
Myelomalacia	4 (7.1)	2 (11.8)	1 (7.1)	0 (0)	1 (11.1)

Unless otherwise indicated, data represent the number of patients with percentages in parenthesis. MRI, magnetic resonance imaging; SD, standard deviation.

TABLE 4. Inter-rater Agreement for Various MRI Involvement Patterns

MRI Findings	Kappa (95% CI)
<i>Brain MRI involvement patterns</i>	
Overall	0.902 (0.900–0.903)
WM involvement patterns	
Extensive and Confluent WM hyperintense lesions on FLAIR	0.863 (0.859–0.867)
Nonconfluent multifocal WM hyperintense lesions on FLAIR	0.910 (0.907–0.914)
Isolated temporal lobe involvement	0.937 (0.934–0.941)
Specific cerebral involvement patterns	
Acute necrotizing encephalopathy	1.000 (0.996–1.004)
PRES	1.000 (0.996–1.004)
Other involvement patterns	
Ischemia	0.977 (0.973–0.981)
Cranial nerve enhancement	0.781 (0.777–0.784)
Isolated hemorrhage	1.000 (0.996–1.004)
Concomitant MRI Findings	
Basal ganglia involvement	0.962 (0.958–0.966)
Brain stem involvement	0.982 (0.978–0.986)
Cerebellum involvement	0.980 (0.986–0.984)
Splenium of corpus callosum involvement	1.000 (0.996–1.004)
Diffusion restriction	0.972 (0.968–0.975)
Hemorrhage	0.915 (0.912–0.918)
Microhemorrhages	0.916 (0.913–0.920)
Intracerebral hematoma	1.000 (0.996–1.004)
Subarachnoid hemorrhage	0.796 (0.796–0.800)
<i>Spinal MRI involvement patterns</i>	
Overall	0.918 (0.915–0.920)
Myelitis	0.945 (0.942–0.949)
Cauda equina and nerve roots enhancement	0.897 (0.893–0.901)
<i>Follow-up MRI involvement patterns</i>	
Overall	0.906 (0.902–0.910)
Resolution	0.899 (0.894–0.904)
Encephalomalacia/atrophy	0.914 (0.909–0.919)
Myelomalacia	0.903 (0.899–0.908)

Data are Kappa values. Data in parentheses are 95% confidence intervals. The κ values were interpreted as follows: 0.00–0.20 = poor agreement; 0.21–0.40 = fair agreement; 0.41–0.60 = moderate agreement; 0.61–0.80 = good agreement; and 0.81–1.00 = perfect agreement.

Our study revealed a diverse range of neuroimaging findings, including non-confluent multifocal hyperintense WM lesions on FLAIR sequences as the most common pattern, followed by ischemia and hemorrhage. These findings are consistent with those of previous studies (20–26) that reported various neurological manifestations in pediatric COVID-19 patients. These findings suggest that COVID-19

may lead to demyelination or inflammatory processes affecting WM tracts in children. The diversity of findings underscores the complex nature of COVID-19's impact on the developing brain.

Ischemia was the second most frequent finding in our cohort, seen in 18.9% of patients. This corroborates the incidence of ischemic stroke reported in previous studies about

TABLE 5. Relation Between Initial MRI Involvement Patterns and Outcomes

MRI involvement patterns	Good outcome (n = 61)	Poor outcome (n = 34)	P-value
<i>Initial brain MRI involvement patterns</i>			
<i>WM involvement patterns</i>			
Confluent multifocal hyperintense WM lesions on FLAIR	10 (16.4)	1 (2.9)	0.090
Nonconfluent multifocal hyperintense WM lesions on FLAIR	28 (45.9)	7 (20.6)	0.014*
Isolated temporal lobe involvement	5 (8.2)	1 (2.9)	0.415
<i>Specific cerebral involvement patterns</i>			
Acute necrotizing encephalopathy	0 (0)	3 (8.8)	0.043*
PRES	2 (3.3)	0 (0)	0.535
<i>Other involvement patterns</i>			
Ischemia	3 (4.9)	15 (44.1)	< 0.001*
Cranial nerve enhancement	7 (11.5)	3 (8.8)	1.000
Isolated cerebral microhemorrhage	0 (0)	1 (2.9)	0.358
<i>Concomitant brain MRI involvement patterns</i>			
Basal ganglia involvement	12 (19.7)	12 (35.3)	0.093
Brain stem involvement	16 (26.2)	10 (29.4)	0.739
Cerebellum involvement	11 (18)	10 (29.4)	0.200
Splenium of corpus callosum involvement	15 (24.6)	10 (29.4)	0.609
<i>Diffusion restriction</i>			
Total Diffusion restriction	20 (32.8)	23 (67.7)	0.002*
Foci of Diffusion restriction with other patterns than infarction	17 (27.9)	8 (23.5)	0.800
Hemorrhage	5 (8.2)	15 (44.1)	< 0.001*
<i>Initial Spinal MRI involvement patterns</i>			
Myelitis	11 (18.0)	4 (11.8)	0.422
Cauda equina enhancement	6 (9.8)	6 (17.6)	0.338

The data represent the number of patients with percentages in parenthesis. FLAIR, fluid-attenuated inversion recovery; MRI, magnetic resonance imaging; PRES, Posterior reversible encephalopathy syndrome; SD, Standard deviation; WM, white matter; *, Statistically significant.

COVID-19 neurological complications in children (27–29). The exact causes of ischemic stroke and thrombotic events in COVID-19 are not fully understood, but they likely involve immune-related mechanisms, inflammation-induced hypercoagulability, viral mimicry, direct viral-induced endotheliitis, and elevated antiphospholipid antibodies (30).

Hemorrhage was observed in 21.1% of the patients in our study. This finding is consistent with that of a previous report by Poyiadji et al. (31), which described intracranial hemorrhage as a rare but severe complication of COVID-19 in adults. The underlying mechanisms of hemorrhage in COVID-19 remain unclear; however, it has been hypothesized that endothelial dysfunction, coagulopathy, or direct viral invasion may contribute to vascular damage (32).

Kremer et al. (23) found extensive WM lesions in patients with severe COVID-19. However, data regarding the prognostic significance of WM changes remain limited, particularly in the pediatric population. Interestingly, non-confluent multifocal WM lesions were associated with better outcomes in our study. This is consistent with the findings of Huang et al. (33), who revealed that WM abnormalities were not related to poorer outcomes, and that the changes in WM tended to be reversible and showed constant recovery over a long period. In contrast, some previous reports (34–36) suggest that WM abnormalities

might be associated with poorer outcomes. Ghaderi et al (34) suggest that WM abnormalities observed in neuroimaging studies of COVID-19 patients may be associated with poorer outcomes. Boito et al. (35) showed that WM lesions are common in the acute/subacute phase of the disease but also persist at follow-up after COVID-19, suggesting that they may be associated with poorer outcomes. Bunkerberg et al. (36) found no association between the severity of the WM lesions and the clinical outcomes. The reasons for the discrepancy between our findings and those of previous studies are likely to be multifactorial. Differences in the study population, MRI timing, imaging protocols, and the classification of WM patterns may have contributed to this discrepancy. Moreover, the underlying etiology and temporal evolution of WM lesions in COVID-19 are complex and may involve inflammatory, ischemic, metabolic, and toxic processes (37). The reasons for this discrepancy require further investigation, but it emphasizes the need for a nuanced approach to interpreting neuroimaging findings in pediatric COVID-19 patients.

Ischemia and hemorrhage were significantly associated with poor outcomes in our study. This is consistent with the findings of Kihira et al. (38), who linked ischemic stroke to severe neurological outcomes in COVID-19 patients. Acute necrotizing encephalopathy was also associated with poor outcomes in our

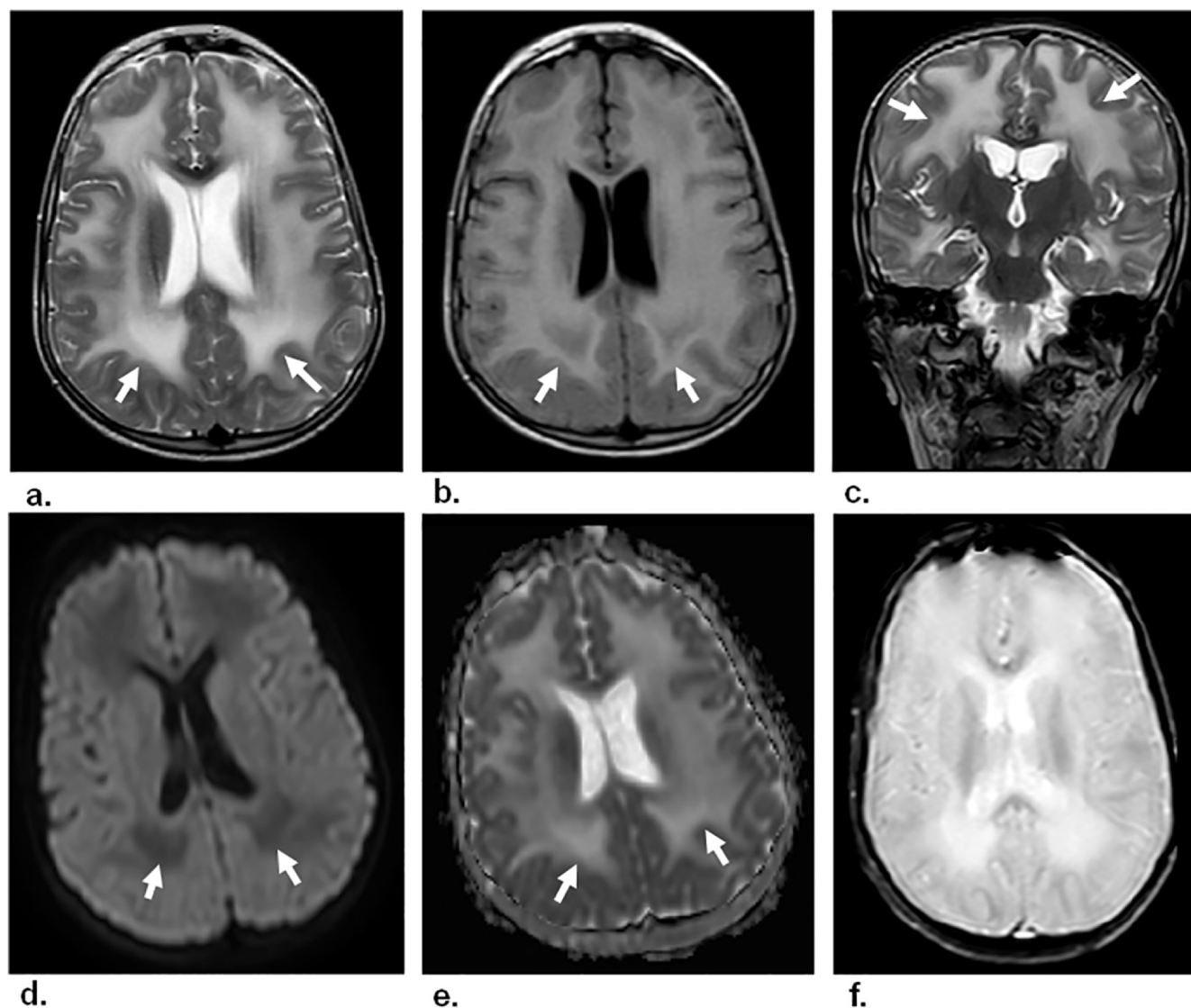


Figure 2. An 11-year-old boy with acute COVID-19 presented with fever, cough, and encephalopathy. **(a)** Axial T2W and **(b)** Axial FLAIR images reveal extensive and confluent areas of high signal intensity in the WM (arrows). **(c)** Coronal T2W image displays the same findings (arrows). **(d)** DWI and **(e)** ADC map show no evidence of restricted diffusion (arrows). **(f)** Axial T2*W image shows no associated hemorrhage.

study, which is consistent with the findings of Lin et al. (39), who highlighted the severity of this rare complication.

The presence of diffusion restriction in nearly half of our patients (45.3%) is consistent with the well-documented association between COVID-19 and ischemic brain injury (40). Diffusion restriction was associated with poor patient outcome. However, when ischemia was excluded, foci with diffusion restrictions associated with other MRI patterns showed no significant difference between good and poor outcomes.

Our study observed cases of myelitis and cauda equina involvement in pediatric COVID-19 patients, which have also been reported to be associated with the disease (41,42). These findings highlight the significance of immune-mediated mechanisms in neurological complications in pediatric COVID-19 patients.

In our study, contrast-enhanced imaging was valuable for detecting cranial neuritis in 10 patients (10.3%) and cauda

equina nerve root enhancement in 12 patients (12.6%). It also helped to exclude the underlying pathology contributing to WM signal changes. Furthermore, DWI was highly informative in identifying and characterizing ischemia in 18 patients (18.9%). Additionally, restricted diffusion foci, in association with other patterns, were observed in 26.3% of patients. These findings corroborate with those reported in previous studies (6,14).

The inclusion of follow-up MRI results in our study provided important insights into the potential outcomes and progression of neuroimaging findings in pediatric COVID-19 patients. The findings from our cohort demonstrated both the reversibility of certain imaging patterns and the potential for the development of encephalomalacia and myelomalacia. Our results align with those of López-Pérez et al. (43), who showed that certain imaging abnormalities associated with pediatric COVID-19 neurological injuries can be reversible.

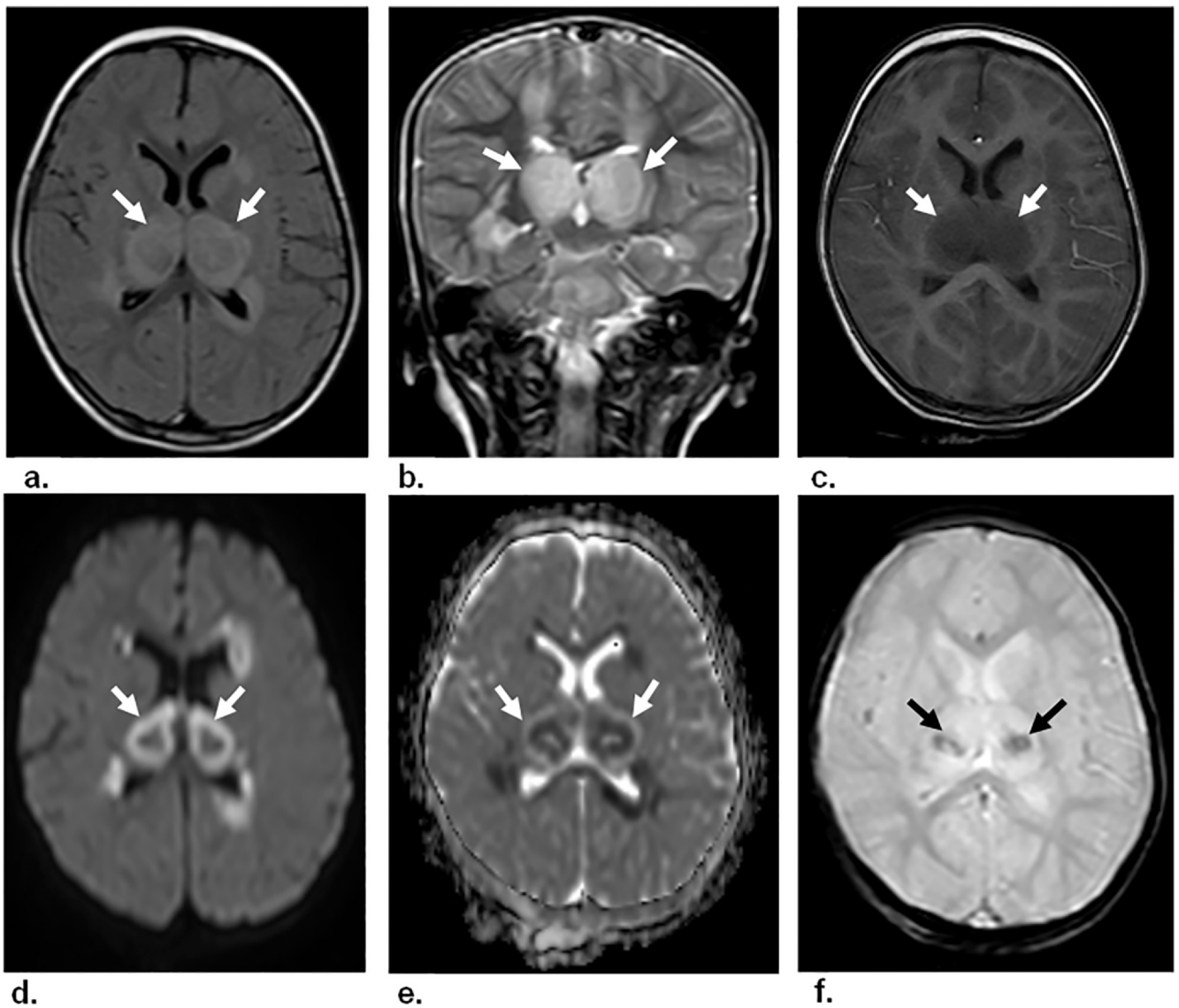


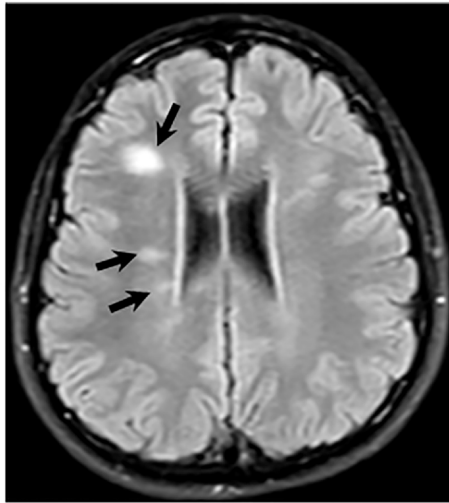
Figure 3. A 12-year-old boy with acute COVID-19 presented with fever and encephalopathy. **(a)** Axial FLAIR and **(b)** Coronal T2W images display bilateral symmetrical thalamic swelling and high signal intensity (arrows). **(c)** Post-contrast T1W image reveals no enhancement (arrows). **(d)** DWI and **(e)** ADC map demonstrate restricted diffusion within the central aspect of the lesion (arrows). **(f)** Axial T2*W image reveals foci of blooming signals denoting hemorrhage (arrows). The MRI findings were consistent with those of acute necrotizing hemorrhagic encephalopathy.

However, the development of encephalomalacia in 23.2% of patients and myelomalacia in 7.1% of patients highlights the potential long-term consequences and tissue damage in some individuals. Studies in adults have shown that MRI abnormalities in severe COVID-19 can resolve, stabilize, or progress (23). Similarly, a study by Lin et al. (39) on acute necrotizing encephalopathy in children with COVID-19 supported the importance of understanding the neurological implications and potential long-term effects of this disease. Furthermore, a study by Boito et al. (35) provided evidence of the persistence and evolution of WM lesions to encephalomalacia, indicating the long-term neurological impact of COVID-19. These findings emphasize the need for follow-up imaging to monitor disease evolution and to guide neurorehabilitation. Overall, our findings

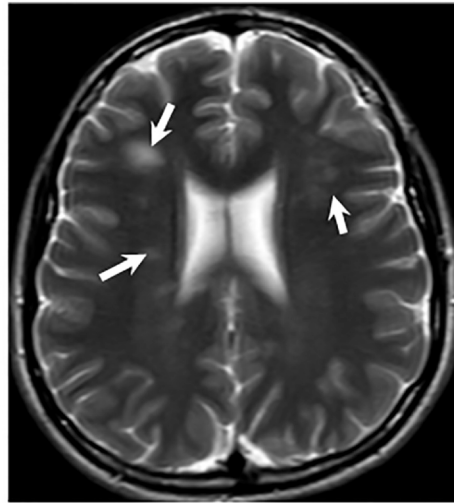
provide initial evidence that while pediatric patients have significant potential for repair and reversibility, COVID-19 neurological insults can also result in permanent sequelae. Follow-up imaging is important to monitor disease evolution and guide neurorehabilitation.

The high inter-rater reliability observed in our study for most MRI patterns confirms the reproducibility of the radiological assessments and supports the validity of neuroimaging findings in COVID-19. Comparatively, these results are largely in concordance with prior studies that highlighted the high IRA among radiologists in interpreting MR neuroimaging findings across various pathologies (44,45).

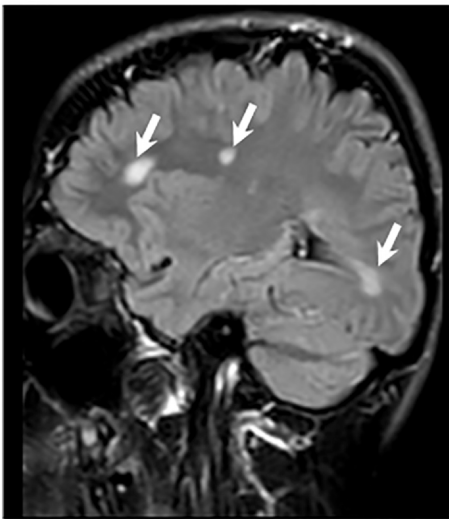
This study had several limitations that should be acknowledged. First, its retrospective design introduced the possibility of



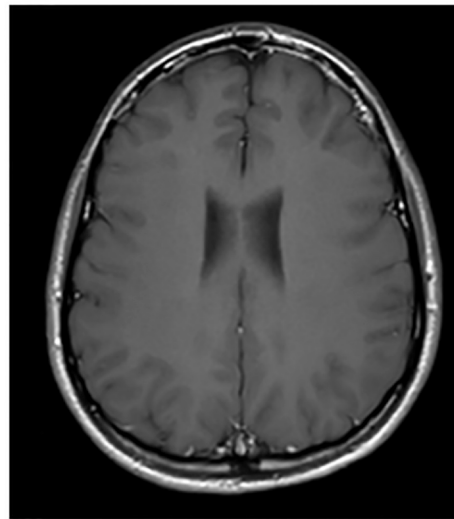
a.



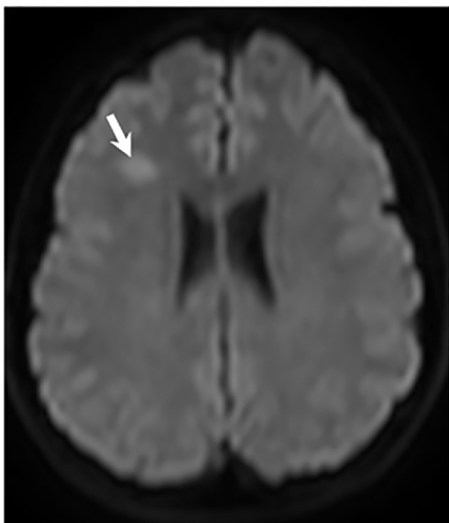
b.



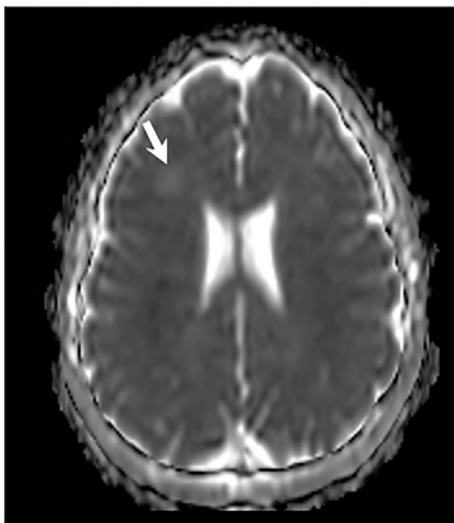
c.



d.



e.



f.

Figure 4. An 8-year-old girl with MIS-C presented with a fever, encephalopathy, and seizures. **(a)** Axial FLAIR, **(b)** T2W, and **(c)** Sagittal FLAIR images illustrate multiple non-confluent ovoid lesions bilaterally located within the frontal, high parietal, and occipital lobes (arrows). **(d)** Axial post-contrast T1W image shows no significant enhancement of the lesions. **(e)** Axial DWI and **(f)** ADC map reveal no restricted diffusion within the lesions. The largest lesion exhibits a relatively high signal intensity on the DWI and ADC map (arrows), whereas the other lesions appear isointense on both sequences.

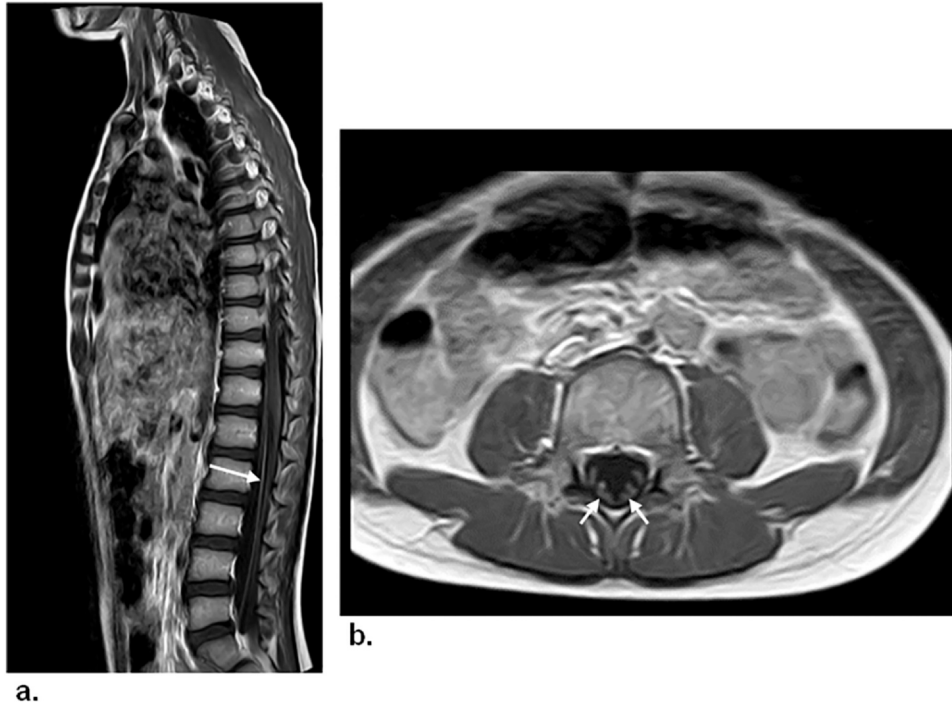


Figure 5. A 6-year-old boy with MIS-C presented with fever, diarrhea, and flaccid paralysis. **(a)** Sagittal and **(b)** Axial post-contrast T1W images reveal enhancement of the cauda equina nerve roots (arrows).

selection bias and limited the ability to establish causal relationships. Second, the relatively small sample size may have restricted the statistical power and generalizability of the findings to the broader pediatric population with COVID-19. Third, this study was conducted at a single center, which may limit the generalizability of the results to other settings. Fourth, incomplete longitudinal analysis due to the lack of follow-up MRI for all patients may have affected the assessment of lesion progression. Fifth, the absence of a long-term follow-up hindered the evaluation of potential delayed or persistent effects. Sixth, the heterogeneity within the clinical groups, particularly the "indeterminate" category, may have confounded the observed associations. Finally, as an observational study, it was not possible to infer causality between the neuroimaging findings and COVID-19 infection.

CONCLUSION

This study yielded several clinically relevant findings regarding MRI patterns in pediatric patients with COVID-19. First, it sheds light on the potential of certain MRI neuroimaging patterns to serve as prognostic indicators of patient outcome. Second, some of these patterns are associated with favorable outcomes, whereas others are linked to poor outcomes. Third,

follow-up MRI scans showed that certain imaging patterns were reversible; however, there was also a risk of developing encephalomalacia and myelomalacia. Finally, these patterns have the potential to influence clinical practice by guiding patient management and treatment decisions. Nevertheless, further research is needed to confirm and build upon these findings, ultimately leading to improved clinical practice and outcomes in pediatric patients with COVID-19.

ETHICAL APPROVAL

Approval was obtained from the Institutional Review Board of Zagazig University in Egypt (approval number: ZU-97/28).

FUNDING

This research was funded by the Deanship of Scientific Research, Najran University, Kingdom of Saudi Arabia, grant number NU/RG/MRC/12/1.

ETHICAL STATEMENT

This retrospective cross-sectional study was approved by the institutional review board (approval number: ZU-97/28)

and conducted under the ethical principles outlined in the Declaration of Helsinki. The requirement for informed consent was waived owing to the retrospective design of the study.

CREDIT AUTHORSHIP CONTRIBUTION STATEMENT

Mohamad Gamal Nada, Yasmin Ibrahim Libda, Yassir Edrees Almalki, Maha Ibrahim Metwally, Mohamad Gamal Nada, and Mohammad Abd Alkhalik Basha designed the study and wrote the manuscript. All authors analyzed and interpreted the data and reviewed and approved the final version of the manuscript.

DECLARATION OF COMPETING INTEREST

The authors of this manuscript declare no relevant conflicts of interest and no relationships with any companies whose products or services may be related to the subject matter of the article.

ACKNOWLEDGMENTS

The authors are thankful to the Deanship of Scientific Research at Najran University for funding this work under the General Research Funding program grant code (NU/RG/MRC/12/1).

INFORMED CONSENT

Written informed consent was waived.

STATISTICS AND BIOMETRY

The corresponding author has great statistical expertise.

METHODOLOGY

- Retrospective.
- Diagnostic study.
- Performed at a single center.

REFERENCES

1. Ludvigsson JF. Systematic review of COVID-19 in children shows milder cases and a better prognosis than adults. *Acta Paediatr* 2020; 109(6):1088–1095.
2. Ellul MA, Benjamin L, Singh B, et al. Neurological associations of COVID-19. *Lancet Neurol* 2020; 19(9):767–783.
3. Lin JE, Asfour A, Sewell TB, et al. Neurological issues in children with COVID-19. *Neurosci Lett* 2021; 743:135567.
4. Ray STJ, Abdel-Mannan O, Sa M, et al. CoroNerve study group. Neurological manifestations of SARS-CoV-2 infection in hospitalised children and adolescents in the UK: a prospective national cohort study. *Lancet Child Adolesc Health* 2021; 5(9):631–641. Epub 2021 Jul 15. Erratum in: *Lancet Child Adolesc Health*. 2021 Jul 28; Erratum in: *Lancet Child Adolesc Health*. 2021 Dec;5(12): e46.
5. Fink EL, Robertson CL, Wainwright MS, et al. Global consortium study of neurologic dysfunction in COVID-19 (GCS-NeuroCOVID) investigators. Prevalence and risk factors of neurologic manifestations in hospitalized children diagnosed with acute SARS-CoV-2 or MIS-C. *Pediatr Neurol* 2022; 128:33–44.
6. Lindan CE, Mankad K, Ram D, et al. ASPNR PECOBIG collaborator group. Neuroimaging manifestations in children with SARS-CoV-2 infection: a multinational, multicentre collaborative study. *Lancet Child Adolesc Health* 2021; 5(3):167–177.
7. Orman G, Desai NK, Kralik SF, et al. Neuroimaging offers low yield in children positive for SARS-CoV-2. *Am J Neuroradiol* 2021; 42(5): 951–954.
8. Riva A, Piccolo G, Balletti F, et al. Acute neurological presentation in children with SARS-CoV-2 infection. *Front Pediatr* 2022; 10:909849.
9. Henderson LA, Canna SW, Friedman KG, et al. American college of rheumatology clinical guidance for multisystem inflammatory syndrome in children associated with SARS-CoV-2 and hyperinflammation in pediatric COVID-19: version 1. *Arthritis Rheumatol* 2020; 72(11): 1791–1805.
10. Jiang L, Tang K, Levin M, et al. COVID-19 and multisystem inflammatory syndrome in children and adolescents. *Lancet Infect Dis* 2020; 20(11):e276–e288.
11. Choi Y, Lee MK. Neuroimaging findings of brain MRI and CT in patients with COVID-19: a systematic review and meta-analysis. *Eur J Radiol* 2020; 133:109393.
12. Liguori L, Liguori G, Liguori A, et al. Neuroimaging findings in a child with severe acute respiratory syndrome coronavirus 2 infection: a case report. *Pediatr Radiol* 2020; 50(12):1995–1997.
13. Abdel-Mannan O, Eyre M, Löbel U, et al. Neurologic and radiographic findings associated with COVID-19 infection in children. *JAMA Neurol* 2020; 77(12):1582.
14. Rastogi S, Gala F, Kulkarni S, et al. Neurological and neuroradiological patterns with COVID-19 infection in children: a single institutional study. *Indian J Radiol Imaging* 2022; 32(4):510–522.
15. Alves de Araujo Junior D, Motta F, Fernandes GM, et al. Neuroimaging assessment of pediatric cerebral changes associated with SARS-CoV-2 infection during pregnancy. *Front Pediatr* 2023; 11:1194114.
16. Chen B, Chen C, Zheng J, et al. Insights into neuroimaging findings of patients with coronavirus disease 2019 presenting with neurological manifestations. *Front Neurol* 2020; 11:593520.
17. Wong AM, Toh CH. Spectrum of neuroimaging mimics in children with COVID-19 infection. *Biomed J* 2022; 45(1):50–62.
18. Casabianca M, Caula C, Titomanlio L, et al. Neurological consequences of SARS-CoV-2 infections in the pediatric population. *Front Pediatr* 2023; 11:1123348.
19. Moriguchi T, Harii N, Goto J, et al. A first case of meningitis/encephalitis associated with SARS-Coronavirus-2. *Int J Infect Dis* 2020; 94:55–58.
20. Helms J, Kremer S, Merdji H, et al. Neurologic features in severe SARS-CoV-2 infection. *N Engl J Med* 2020; 382(23):2268–2270.
21. Bahrani B, Mehdizadeh S, Hamidi A, et al. A review of neuroradiological abnormalities in patients with coronavirus disease 2019 (COVID-19). *Neuroradiol J* 2022; 35(1):3–24.
22. Paterson RW, Brown RL, Benjamin L, et al. The emerging spectrum of COVID-19 neurology: clinical, radiological and laboratory findings. *Brain* 2020; 143(10):3104–3120.
23. Kremer S, Lersy F, de Sèze J, et al. Brain MRI findings in severe COVID-19: a retrospective observational study. *Radiology* 2020; 297(2): E242–E251.
24. Kandemirli SG, Dogan L, Sarikaya ZT, et al. Brain MRI findings in patients in the intensive care unit with COVID-19 infection. *Radiology* 2020; 297(1):E232–E235.
25. Dixon L, Varley J, Gontsarova A, et al. COVID-19-related acute necrotizing encephalopathy with brain stem involvement in a patient with aplastic anemia. *Neurol Neuroimmunol Neuroinflamm* 2020; 7(5):e789.
26. Coolen T, Lolli V, Sadeghi N, et al. Early postmortem brain MRI findings in COVID-19 non-survivors. *Neurology* 2020; 95(14):e2016–e2027.
27. LaRovere KL, Riggs BJ, Poussaint TY, et al. Neurologic involvement in children and adolescents hospitalized in the United States for COVID-19 or multisystem inflammatory syndrome. *JAMA Neurol* 2021; 78(5): 536–547.

28. Sánchez-Morales AE, Urrutia-Osorio M, Camacho-Mendoza E. Neurological manifestations temporally associated with SARS-CoV-2 infection in pediatric patients in Mexico (et). *Childs Nerv Syst* 2021; 37(7):2305–2312.
29. DosSantos MF, Devalle S, Aran V, et al. Neuromechanisms of SARS-CoV-2: a review. *Front Neuroanat* 2020; 14:37.
30. Tiwari L, Shekhar S, Bansal A, et al. COVID-19 associated arterial ischaemic stroke and multisystem inflammatory syndrome in children: a case report. *Lancet Child Adolesc Health* 2021; 5(1):88–90.
31. Poyiadji N, Shahin G, Noujaim D, et al. COVID-19-associated acute hemorrhagic necrotizing encephalopathy: imaging features. *Radiology* 2020; 296(2):E119–E120.
32. Katz JM, Libman RB, Wang JJ, et al. Cerebrovascular complications of COVID-19. *Stroke* 2020; 51(9):e227–e231.
33. Huang S, Zhou Z, Yang D, et al. Persistent white matter changes in recovered COVID-19 patients at the 1-year follow-up. *Brain* 2022; 145(5):1830–1838.
34. Ghaderi S, Olfati M, Ghaderi M, et al. Neurological manifestation in COVID-19 disease with neuroimaging studies. *Am J Neurodegener Dis* 2023; 12(2):42–84.
35. Boito D, Eklund A, Tisell A, et al. MRI with generalized diffusion encoding reveals damaged white matter in patients previously hospitalized for COVID-19 and with persisting symptoms at follow-up. *Brain Commun* 2023; 5(6):fcad284.
36. Bungenberg J, Humkamp K, Hohenfeld C, et al. Long COVID-19: objectifying most self-reported neurological symptoms. *Ann Clin Transl Neurol* 2022; 9(2):141–154.
37. Ferrarese C, Silani V, Priori A, et al. Italian Society of Neurology (SIN). An Italian multicenter retrospective-prospective observational study on neurological manifestations of COVID-19 (NEUROCOVID). *Neurol Sci* 2020; 41(6):1355–1359.
38. Kihira S, Schefflein J, Mahmoudi K, et al. Association of coronavirus disease (COVID-19) with large vessel occlusion strokes: a case-control study. *Am J Roentgenol* 2021; 216(1):150–156.
39. Lin X, Wang Y, Li X, et al. Acute necrotizing encephalopathy in children with COVID-19: a retrospective study of 12 cases. *Front Neurol* 2023; 14:1184864.
40. Caroli A, Capelli S, Napolitano A, et al. Brain diffusion alterations in patients with COVID-19 pathology and neurological manifestations. *Neuroimage Clin* 2023; 37:103338.
41. Toscano G, Palmerini F, Ravaglia S, et al. Guillain-Barré syndrome associated with SARS-CoV-2. *N Engl J Med* 2020; 382(26):2574–2576.
42. Alberti P, Beretta S, Piatti M, et al. Guillain-Barré syndrome related to COVID-19 infection. *Neurol Neuroimmunol Neuroinflamm* 2020; 7(4):e741.
43. López-Pérez BJ, Cruz-Chávez DA, Solórzano-Gómez E, et al. Neurological manifestations in pediatric patients hospitalized for COVID-19: experiences of the National Medical Center "20 de Noviembre" in Mexico City. *Children (Basel)* 2022; 9(5):746.
44. van der Ende NAM, Luijten SPR, Kluijtmans L, et al. Interobserver agreement on intracranial hemorrhage on magnetic resonance imaging in patients with ischemic stroke. *Stroke* 2023; 54(6):1587–1592.
45. Lecler A, Cotton F, Lersy F, et al. SFNR's COVID study group. Abnormal MRI findings of the orbital or visual pathways in patients with severe COVID-19: observations from the French multicenter COVID-19 cohort. *J Neuroradiol* 2021; 48(5):331–336.